# Experimental structure factor of solutions of randomly branched polymers

F. Schosseler, M. Daoud, L. Leibler

*J. Phys. France* **51** (1990) 2373-2385 15 OCTOBRE **1990,** PAGE 2373

Classification
*Physics Abstracts*
82.70G — 36.20C — 64.60F

# Experimental structure factor of solutions of randomly branched polymers

F. Schosseler ([1]), M. Daoud ([2]) and L. Leibler ([3])

([1]) Institut Charles Sadron, 6 rue Boussingault, 67083 Strasbourg Cedex, France
([2]) Laboratoire Léon Brillouin (*), CEN Saclay, 91191 Gif-sur-Yvette, France
([3]) Laboratoire de Physicochimie Théorique, E.S.P.C.I., 10 rue Vauquelin, 75231 Paris Cedex 05, France

(*Received 11 April 1990, accepted in final form 27 May 1990*)

**Résumé.** — Nous avons effectué des expériences de diffusion de rayonnement sur des solutions diluées de phases sol produites lors d'une réaction de gélification. La comparaison des facteurs de structure mesurés sur des échantillons fractionnés ou non fractionnés permet de séparer les effets de dispersion en tailles et les propriétés conformationnelles des espèces ramifiées. Les résultats montrent que, dans une solution diluée, le comportement de ces objets est plutôt en accord avec celui attendu pour des amas de percolation gonflés.

**Abstract.** — We have performed scattering experiments on dilute solutions of polydisperse and fractionated sol phases obtained in a gelation process. The comparison of the structure factors allows one to separate size polydispersity effects and conformational properties of the branched species. Our results show that their behavior in solution agrees rather well with the one expected for swollen percolation clusters.

## Introduction.

During the last decade the structure of branched growing aggregates has been the subject of a large number of experimental and theoretical studies [1]. The large aggregates that are built in a given growth process are characterized by the same decay of the pair correlation function. Scattering experiments measure the Fourier transform of the pair correlation function and thus are a convenient method to study growth processes.

Gelation is a particular class of growth processes in which the growing clusters interpenetrate each other and finally constitute a macroscopic object which spans the whole reaction bath [1, 2]. In this process, the interactions between the growing clusters are important and screen the intramolecular interactions beyond a distance that depends on the concentration in

(*) Laboratoire commun CEA-CNRS.

the reaction bath. Thus the branched molecules constituting the sol phase are more compact than the branched objects obtained from aggregation in a dilute solution. One striking feature of the sol phase is the huge size polydispersity of the growing clusters. At the gel point, all sizes of clusters are present in the reaction bath, from the constitutive units to the macroscopic infinite cluster. The size distribution function of these objects obey a scaling form and the physical properties are those of individual branched molecules averaged over this size distribution function [2-12].

This paper reports on the conformational properties of randomly branched molecules synthesized by crosslinking of pre-existing linear chains in solution. This reaction allows one to obtain gels but, for all the samples studied here, the reaction has been stopped before the gel point is reached. Fractions with low polydispersities have been prepared by precipitation fractionation from a pregel sample. We have measured by small angle neutron scattering (SANS) and light scattering (LS) techniques the intensity scattered from polydisperse and fractionated samples. By comparison of their structure factors measured on length scales between the monomer size and the radius of gyration, we can separate polydispersity effects and gain information about the conformation in solution of both the branched molecules and the linear precursor chains. The same method has already been used by Bouchaud *et al.* [10] to study the clusters obtained by the polycondensation of small molecules.

**Theoretical background.**

In recent years fractals have become a familiar concept in a wide range of physical phenomena [1, 13, 14]. Fractal aggregates have a self-similar structure in a large range of length scales. They are invariant by dilation : pictures of an aggregate taken with different magnifying lenses look the same. This can be expressed mathematically by a power law decay [5, 15] for the pair correlation function $g(r)$ defined as the monomer concentration at a distance $r$ from a given monomer. For a finite fractal, this algebraic decay is valid for distances between the size $a$ of the constituting units and a typical size roughly equal to the radius of gyration $R$ of the aggregate. Therefore we have :

$$g(r) \sim r^{D-d} h(r/R) \tag{1}$$

where $D$ is the fractal dimension, $d$ the space dimension and $h(x)$ a crossover function : for $x \ll 1$, $h(x) \sim 1$ and for large $x$, $h(x)$ decays faster than any power law. Upon spatial integration of equation (1), one obtains a very simple relationship between the mass $M$ and the radius of gyration $R$ of a fractal aggregate :

$$M \sim R^D . \tag{2}$$

The fractal dimension $D$ is always smaller than the space dimension and equations (1) and (2) reflect the presence in the aggregate of self-similar defects that are responsible for its smaller density.

In highly diluted solutions one can approximate the total scattered intensity by the sum of the intensities scattered from each aggregate. Then the intensity $S_M(q)$ scattered from a set of statistical fractals with the same mass $M$ is proportional to the Fourier transform of equation (1) :

$$S_M(q) = \frac{nM}{V} \int \frac{\sin(qr)}{qr} g(r) r^2 \mathrm{d}r \tag{3}$$

where $n$ is the number of aggregates in the scattering volume $V$. Using the properties of the

crossover function $h(x)$, one defines the intermediate scattering regime ($R^{-1} \ll q \ll a^{-1}$) where the scattered intensity decays as a simple power law :

$$S_M(q) \sim C q^{-D} \tag{4}$$

where $C$ is the concentration and $q$ denotes the scattering wave vector.

Equations (1), (2) and (4) are three widely used definitions of the fractal dimension $D$. A simple well-known fractal is a long polymer chain in a good solvent whose fractal dimension is very close to 5/3.

For a set of fractal clusters with different molecular weights the preceding relations are modified by polydispersity effects as emphasized earlier by Daoud *et al.* [4] and Martin *et al.* [5]. The size distribution function of the largest clusters obtained in a gelation reaction is usually written in the vicinity of the gel point as a scaling equation [3] :

$$P(M, \varepsilon) \sim M^{-\tau} f(M/M^*) \tag{5}$$

where $P(M, \varepsilon)\, \mathrm{d}M$ is the number of branched molecules with a molecular weight between $M$ and $M + \mathrm{d}M$, when the relative distance to the gel point is $\varepsilon = (1 - p/p_c)$. Here $p$ is the extent of the reaction and $p_c$ the $p$ value at the gel point. The function $f(x)$ is a crossover function with usual behaviour ($f(x) \sim 1$ for $x \ll 1$ and $f(x) \ll 1$ for $x \gg 1$). In the scaling equation (5) the distribution function $P(M, \varepsilon)$ depends on the extent of the reaction through the single quantity $M^*$. The cut-off molecular weight $M^*$ characterizes the spreading of the size distribution function and diverges at the gel point where the polydispersity is infinite :

$$M^* \sim \varepsilon^{-1/\sigma}. \tag{6}$$

Thus, at the gel point, $P(M, \varepsilon = 0)$ decays as a simple power law :

$$P(M, \varepsilon = 0) \sim M^{-\tau}. \tag{7}$$

The exponents $\sigma$ and $\tau$ that appear in equations (5) to (7) are critical exponents, whose values can be calculated in the Flory-Stockmayer approximation [16] ($\sigma = 1/2$, $\tau = 5/2$) or in the percolation model [3] ($\sigma \cong 0.46$, $\tau \cong 2.2$).

The total intensity scattered from a polydisperse sample in dilute solution is obtained by a straightforward generalization [5] of equation (3) :

$$S(q) = \int \mathrm{d}M\, P(M, \varepsilon) \frac{M}{V} \int \frac{\sin(qr)}{qr} r^{D-d} h(r/M^{1/D})\, r^{d-1}\, \mathrm{d}r. \tag{8}$$

In the small $q$ range, equation (8) reduces to the usual Guinier expansion of the scattered intensity :

$$S(q) = C M_W \left(1 - \frac{q^2}{3} R_z^2\right) \tag{9}$$

where $C$, $M_W$ and $R_z^2$ are respectively the concentration, the weight averaged molecular weight and the $z$-averaged radius of gyration of the sample :

$$C = \frac{1}{V} \int \mathrm{d}M\, M P(M, \varepsilon) \tag{10}$$

$$M_W = \frac{\int dM\, M^2 P(M, \varepsilon)}{\int dM\, MP(M, \varepsilon)} \tag{11}$$

$$R_z^2 = \frac{\int dM\, M^2 M^{2/D} P(M, \varepsilon)}{\int dM\, M^2 P(M, \varepsilon)} . \tag{12}$$

Using equation (5) into (11) and (12), it is easy to obtain the scaling relation between $M_W$ and $R_z^2$ [3-5] :

$$M_W \sim (R_z^2)^{D(3-\tau)/2} . \tag{13}$$

In the intermediate scattering regime defined now by $R_z^{-1} \ll q \ll a^{-1}$, the scattered intensity obtained from (8) still decays as a power law but with a different exponent :

$$S(q) \sim C q^{-D(3-\tau)} . \tag{14}$$

The comparison of relations (13) and (14) with equations (2) and (4) shows that the effect of the polydispersity is to replace the true fractal dimension $D$ by a smaller apparent fractal dimension $D_{app} = D(3 - \tau)$.

**Experimental part.**

Pregel samples are prepared by $\gamma$-irradiation induced crosslinking of polystyrene chains in cyclopentane. The temperature during irradiation is kept to 22 ± 1 °C which is slightly above the theta temperature of the PS-$C_5H_{10}$ system. The concentration in the reaction bath (0.1 g/cm$^3$) is close to the overlap concentration of the chains.

The sample preparation follows the procedure already described [6, 9]. The extent of the reaction is controlled by the irradiation dose. Free radicals are induced by $\gamma$-rays on the chains and on the solvent molecules. Then crosslinking comes about by a combination of neighbouring radicals on the chains. Direct radiolysis of polystyrene chains in bulk is known to induce approximately 1 chain scission for 10 crosslinking reactions. But here solvent radiolysis is the dominant process in the polymer solution because the polymer weight fraction is only about 0.1. Therefore most of the radicals created on polystyrene chains are obtained by transfer from the free radicals induced on solvent molecules. This process reduces to a large extent the chain scission that is essentially due to the direct radiolysis of the chains. In fact no chain scission is observed in size exclusion chromatography experiments.

Small angle neutron scattering experiments have been performed on the PACE spectrometer in Laboratoire Léon Brillouin during two different runs.

During the first one the intensity scattered from dilute solutions of polydisperse branched samples has been measured as a function of the extent of the reaction. The samples used in this experiment have already been studied by light scattering [9] and size exclusion chromatography coupled with light scattering [6] (SEC-LALLS) techniques. They are prepared from linear hydrogenated PS chains with weight averaged molecular weight $M_W \simeq 55\,000$ and polydispersity index 1.2. Their characteristics are listed in table I.

Small values of the momentum transfer range, $4.71 \times 10^{-3} \leqslant q(\text{Å}^{-1}) \leqslant 5 \times 10^{-2}$, have been obtained by combining a large value ($\lambda = 16$ Å) for the wavelength of the incident

Table I. — *Characteristics of the polydisperse samples. The pregels with no concentration C indicated have not been studied by* SANS *technique. Sample* 450 *contains only the linear precursor chains. Error bars correspond to a* 68 % *confidence interval for the experimental values.*

| Sample | $M_W \times 10^{-5}$ | $R_Z$ (Å) | $C \times 10^3$ (g/cm$^3$) | $D_{app}$ |
|---|---|---|---|---|
| 450-0 | 0.55 ± 0.03 | 85 ± 10 | 2.82 | — |
| 450-49 | 1.17 ± 0.06 | 160 ± 30 | 3.65 | — |
| 450-50 | 1.65 ± 0.1 | 163 ± 40 | — | — |
| 450-51 | 2.7 ± 0.3 | 220 ± 30 | — | — |
| 450-56 | 3.95 ± 0.4 | 277 ± 20 | — | — |
| 450-54 | 5.3 ± 0.3 | 360 ± 10 | 1.58 | 1.37 ± 0.09 |
| 450-53 | 9.3 ± 0.5 | 465 ± 10 | 1.44 | 1.39 ± 0.06 |
| 450-57 | 9.9 ± 0.5 | 495 ± 15 | — | — |
| 450-55 | 18.3 ± 1.2 | 710 ± 10 | 1.12 | 1.49 ± 0.06 |
| 450-182 | 22 ± 3 | 840 ± 40 | 0.99 | 1.57 ± 0.05 |
| 450-180 | 25 ± 4 | 930 ± 50 | — | — |
| 450-178 | 37 ± 2 | 1 100 ± 20 | 0.61 | 1.47 ± 0.07 |
| 450-63 | 115 ± 10 | 1 900 ± 50 | 0.44 | 1.61 ± 0.1 |
| 450-61 | 141 ± 30 | 2 200 ± 100 | 0.62 | 1.73 ± 0.11 |

neutrons and a distance between the sample and the detector equal to 2.5 m. The samples have been diluted in $C_6D_6$ at concentrations around $10^{-3}$ g/cm$^3$ (see Tab. I). As a sample background we have used pure $C_6D_6$, thus neglecting the incoherent scattering from hydrogenated polystyrene. With the small polymer concentration of the samples, this extra incoherent scattering is only about 4 % of the total incoherent scattering of the sample background.

The data treatment has been made according to a standard procedure. All spectra have been first corrected from the electronic noise measured with a Cd plate in place of the sample and then corrected for sample thickness and absorption. After the subtraction of the intensity scattered by the background sample, normalization to the unit incident flux, geometrical factors and detector cells efficiency corrections have been performed by using the incoherent scattering of $H_2O$, corrected for the scattering of the empty cell. The data are put on an

absolute scale by introducing the differential cross section per unit volume of $H_2O$. We have used the values listed in table II as they are provided by the utilitary program WATWET (ILL, Grenoble), that gives a polynomial interpolation through experimental values measured by R. C. Oberthür. We thus obtain the absolute scattered intensity $I(q)$ (in barns), which is proportional to the structure factor $S(q)$. The proportionality constant $K$ is given by the contrast between the polymer and the solvent. $K$ has been measured by using the linear precursor sample as a standard since, for this low molecular weight sample, the scattering function is measured in the Guinier range. By extrapolating the data to the zero wavevector value in Zimm representation we get :

$$\frac{KC}{I(q)}\Big|_{q\to 0} = \frac{1}{M_W} + 2A_2C \tag{15}$$

where $C$ is the polymer concentration and $A_2$ the second virial coefficient of PS chains with molecular weight $M_W \simeq 55\,000$ in $C_6D_6$. In fact we have used for $A_2$ the corresponding value in $C_6H_6$, $A_2 \simeq 6.44 \times 10^{-4}$ cm$^3$/g$^2$, which should be very close to the true value. Thus we are able to measure the absolute structure factor $S(q)$ for all the samples.

Figure 1 shows the SANS results for some of the samples together with light scattering data obtained from previous experiments on the same samples diluted in toluene [9]. The light scattering data points are obtained from extrapolation to zero concentration whereas neutron scattering data are obtained by simply dividing the scattered intensity by the polymer concentration. However the agreement between the two data sets is quite good. In fact neglecting the virial terms for high molecular weight branched samples introduces only a small error since the polymer concentration (see Tab. I) and second virial coefficient (around $10^{-5}$ cm$^3$/g$^2$) are small for these samples. Thus the virial term in equation (15) is only about 1 % of the term $M_W^{-1}$.

In the second experiment the intensity scattered from different fractions of the same branched sample has been measured as a function of molecular weight. A polydisperse sample has been prepared as usually from the same precursor chains and then separated into fractions by using precipitation fractionation. These fractions have been characterized in toluene by a light scattering technique. The apparatus is an AMTEC photogoniometer with incident light supplied by a He-Ne laser ($\lambda = 6\,328$ Å) and scattering angles comprised between 10° and 160°. Values of $M_W$ and $R_z$ are listed in table III and plotted in figure 2. Table III also gives for each fractionated sample its approximate corresponding weight fraction in the polydisperse sample.

As in the first experiment the samples have been diluted in $C_6D_6$ for SANS experiments (see concentrations in Tab. III). In order to improve the counting rates, scattering cells with a 10 mm optical path (instead of 5 mm in the first experiment) have been used. Two different incident neutron wavelengths have been used, $\lambda = 7.46$ Å and $\lambda = 15.5$ Å, with a sample detector distance equal to 2.5 m. The corresponding $q$ range for the two configurations is $1.01 \times 10^{-2} \leqslant q(\text{Å}^{-1}) \leqslant 1.07 \times 10^{-1}$ and $4.86 \times 10^{-3} \leqslant q(\text{Å}^{-1}) \leqslant 5.16 \times 10^{-2}$, respectively. Scattered intensity data, corrected as in the first experiment, are shown in figure 3 together with the light scattering results.

**Results and discussion.**

Figures 1 and 3 show that there is a $q$ range where the scattered intensities tend to be insensitive to the molecular weight of the samples as the molecular weight increases. Moreover, the extension of this $q$ range increases with the molecular weight. This is the expected behavior for fractal systems in the intermediate scattering regime (Eqs. (4) and (14)).

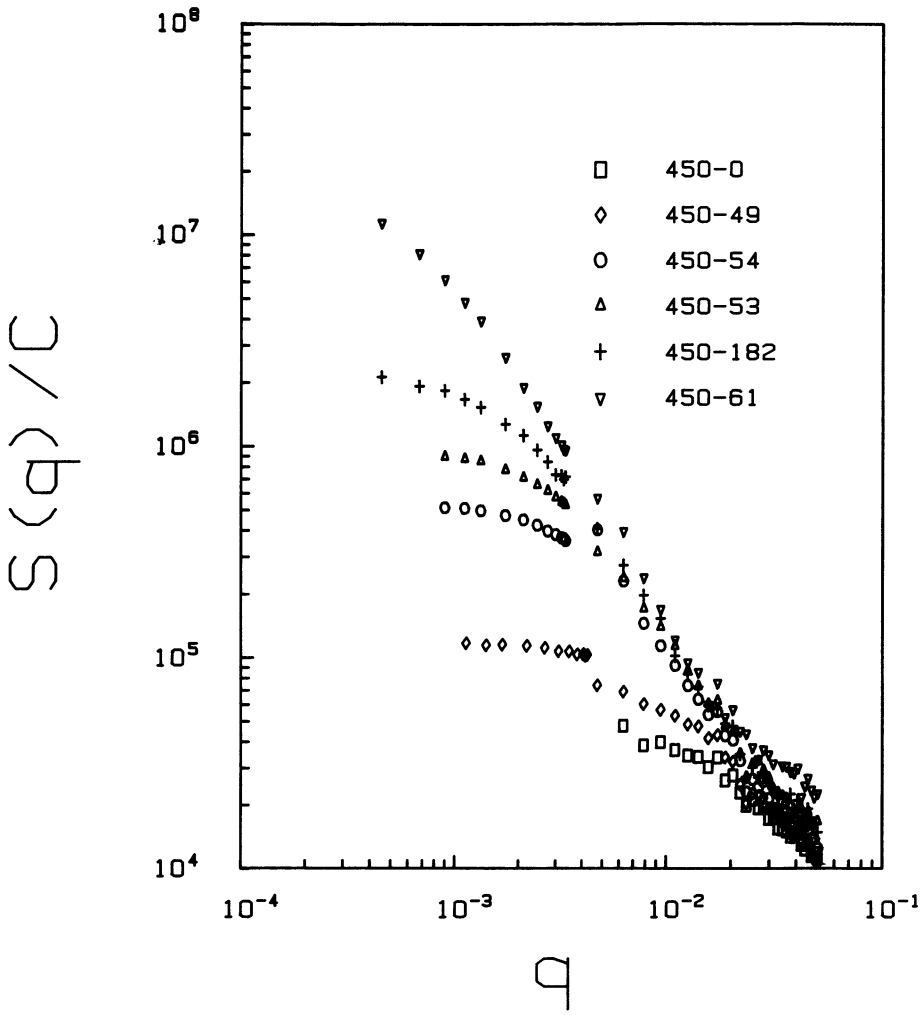


Fig. 1. — Intensities scattered from polydisperse pregels with different weight averaged molecular weight $M_W$. Sample 450-0 contains only the linear precursor chains. The extrapolation to zero $q$ value corresponds to $M_W$ for each sample. Data points for $q < 5 \times 10^{-3}$ have been obtained by the light scattering technique.

Table II. — *Effective differential incoherent scattering cross section of* $H_2O$ *for different wavelengths of the incident neutrons.*

| $\lambda$ (Å) | 7.46 | 15.5 | 16 |
|---|---|---|---|
| $\left.\frac{d\Sigma}{d\Omega}\right\|^{1\text{ mm}}_{H_2O}$ ($cm^{-1}$) | 0.900 | 1.117 | 1.13 |

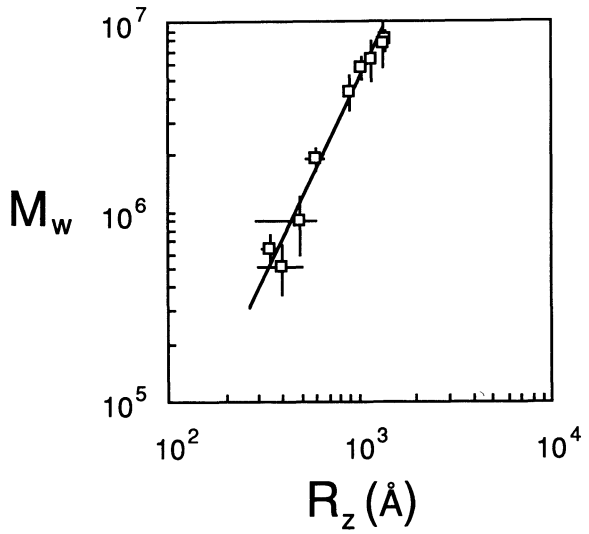


Fig. 2. — Variation of the weight averaged molecular weight of the fractions as a function of their radius of gyration (Tab. III).

It is interesting to compare the intensities $S(q)/C$ scattered from polydisperse and fractionated samples with the same weight averaged molecular weight (Fig. 4). At small $q$ values, their scattered intensities are the same since $\left(\frac{S(q)}{C}\right)_{q\to 0} = M_W$. Then, in the Guinier range, the decrease in the scattered intensities is given by the $z$-averaged radius of gyration (Eq. (9)), which is larger in the polydisperse sample than in the fractionated sample. Thus the scattered intensity decreases faster for the polydisperse sample. On the other hand, in the intermediate scattering regime, the intensity scattered from the fractionated sample decreases faster since $D$ is larger than $D_{app}$. Finally in the high $q$ range, corresponding to the intermediate scattering regime for the linear precursor chains ($R_0^{-1} < q < a^{-1}$, a being the statistical length of the chains), the scattered intensities become the same for the two samples. In figure 4 the difference between the two samples in this $q$ range is an artefact due to the fact that the intensity scattered from sample 450-55 has been measured in the first experiment (small signal-to-noise ratio). In the second experiment however (Fig. 3), no difference is detectable in the high $q$ range between the polydisperse sample 450-214 and the fractions.

Thus three different scattering regimes separated by crossover regions can be distinguished in the scattered intensities of the samples : the Guinier range, the intermediate scattering regime for the branched species and the intermediate scattering regime for the linear precursor chains. Each regime can be observed only over a limited $q$ range, typically less than one decade. Therefore the measurement of accurate values for the exponents $D$ and $D_{app}$ is not easy. This is particularly true for the polydisperse samples because the transition between the different regimes is smoothed off by the polydispersity (Fig. 4).

Table I lists the values of $D_{app}$ determined for the polydisperse samples. These values have been obtained from a weighted least squares fit of the scattered intensities in the $q$ range $4.7 \times 10^{-3} < q$ (Å$^{-1}$) $< 2 \times 10^{-2}$. For the fractionated samples, the values of $D$ listed in table III have been determined in the same way in nearly the same $q$ range ($5 \times 10^{-3} < q$ (Å$^{-1}$) $< 2 \times 10^{-2}$). Considering that the radius of gyration of the precursor chains is $R_0 \simeq 85$ Å, this $q$ range fulfills the condition $R_z^{-1} < q < R_0^{-1}$ for all the

Table III. — *Characteristics of the polydisperse sample* 450-214 *and its fractions. Same remarks as for table I.*

| Sample | Weight fraction % | $M_W \times 10^{-5}$ | $R_Z$ (Å) | $C \times 10^3$ (g/cm$^3$) | $D$ | $D_\ell$ |
|---|---|---|---|---|---|---|
| 450-214 | 100 | 11.6 ± 1.5 | 610 ± 30 | 3.46 | 1.50 ± 0.03 (*) | 1.67 ± 0.02 |
| 450-214 F1 | 3 | 80 ± 10 | 1 390 ± 40 | — | — | — |
| 450-214 F2 | 2.5 | 77 ± 20 | 1 350 ± 30 | 2.17 | 1.99 ± 0.05 | 1.62 ± 0.03 |
| 450-214 F3 | 6 | 57 ± 8 | 1 030 ± 20 | 2.49 | 2.12 ± 0.06 | 1.76 ± 0.04 |
| 450-214 F4 | 6.5 | 63 ± 15 | 1 170 ± 40 | 2.33 | 2.11 ± 0.06 | 1.72 ± 0.03 |
| 450-214 F5 | 3 | 43 ± 9 | 905 ± 20 | 2.58 | 2.07 ± 0.06 | 1.72 ± 0.04 |
| 450-214 F6 | 5 | 19 ± 2.5 | 590 ± 60 | 2.62 | 2.00 ± 0.07 | 1.72 ± 0.04 |
| 450-214 F7 | 2.5 | 9 ± 3 | 490 ± 100 | — | — | — |
| 450-214 F8 | 6 | 6.4 ± 1.2 | 340 ± 30 | — | — | — |
| 450-214 F9 | 5 | 5.2 ± 1.5 | 400 ± 100 | — | — | — |
| 450-214 F10 | 7.5 | — | — | — | — | — |
| 450-214 F11 | 43 | 1.3 ± 0.2 | 530 ± 50 | — | — | — |
| 450-0 | — | 0.55 ± 0.03 | 85 ± 10 | 2.54 | — | 1.56 ± 0.03 |

(*) This value corresponds in fact to $D_{app}$.

samples studied here. In the high $q$ range, $0.03 < q$ (Å$^{-1}$) $< 0.08$, corresponding to the intermediate scattering regime for the linear chains, the same fitting procedure has given the $D_\ell$ values listed in table III.

A close inspection of the values of $D_{app}$, $D$ and $D_\ell$ shows some scattering in the results, especially in the first experiment where the signal-to-noise ratio was small. To decrease the statistical errors, we have used in the second experiment a longer optical path for the scattering cells and slightly higher polymer concentrations. In previous similar experiments [10], some dependence of the exponent values on the polymer concentration has been reported. Clearly the accuracy in the data (Tabs. I and III) is not high enough to detect such an effect here : there is no systematic correlation between the variation of the exponents and the concentration of the samples. Therefore the values in tables I and III have been averaged to obtain the mean values $\bar{D}_{app} = 1.53 \pm 0.15$, $\bar{D} = 2.06 \pm 0.10$ and $\bar{D}_\ell = 1.70 \pm 0.05$, where the error bars reflect the scattering of the data.

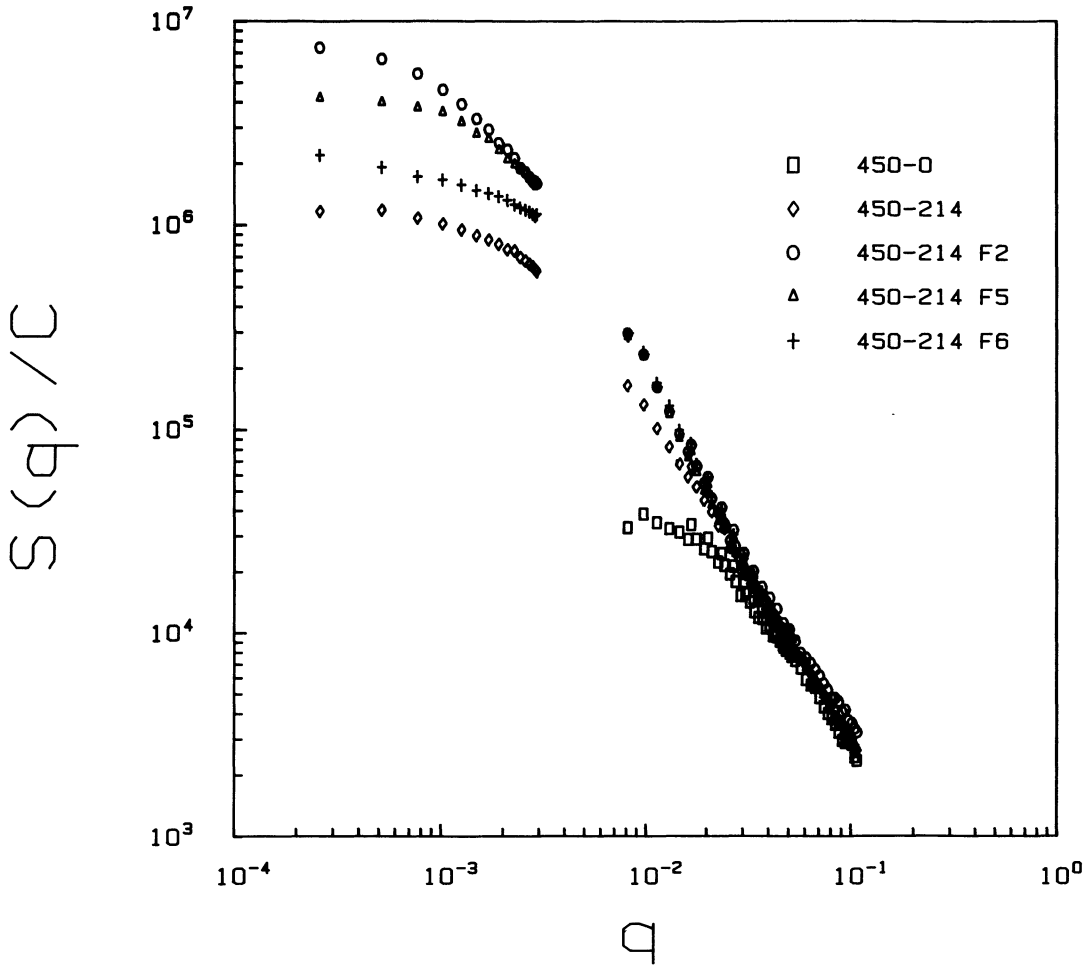


Fig. 3. — Same as figure 1 for the pregel 450-214 and its fractions.

From the light scattering results plotted in figure 2 and equation (2), we obtain the value $D_{LS} = 2.04 \pm 0.15$ which is in agreement with $\bar{D}$ measured in the SANS experiments. On the other hand, the value $D^{-1}_{app,LS} = 0.58 \pm 0.06$, deduced earlier [9] from light scattering experiments on the polydisperse samples, appears to be not well consistent with $\bar{D}_{app}$. However in reference [9] the fit of the data was done with a simple least squares adjustment that does not take into account the error bars associated with the experimental values. Therefore we have replotted in figure 5 these previous results together with some new data (corresponding to samples 450-178 and 450-61 in Tabl. I). A weighted least squares fit across the whole set of data gives $D_{app,LS} = 1.67 \pm 0.04$, slightly different from the previous determination. If we do not consider the two points corresponding to the higher molecular weights ($M_W > 10^7$), we obtain a smaller value $D_{app,LS} = 1.61 \pm 0.04$ that is in better agreement with $\bar{D}_{app}$. The latter procedure could be justified by the fact that the accuracy on the values of $M_W$ and $R_Z$ measured by light scattering techniques becomes rather poor for very large molecules. Nevertheless in the following we shall use the first value of $D_{app,LS}(1.67)$, keeping in mind that the error bars might be larger than those given by the fitting procedure.

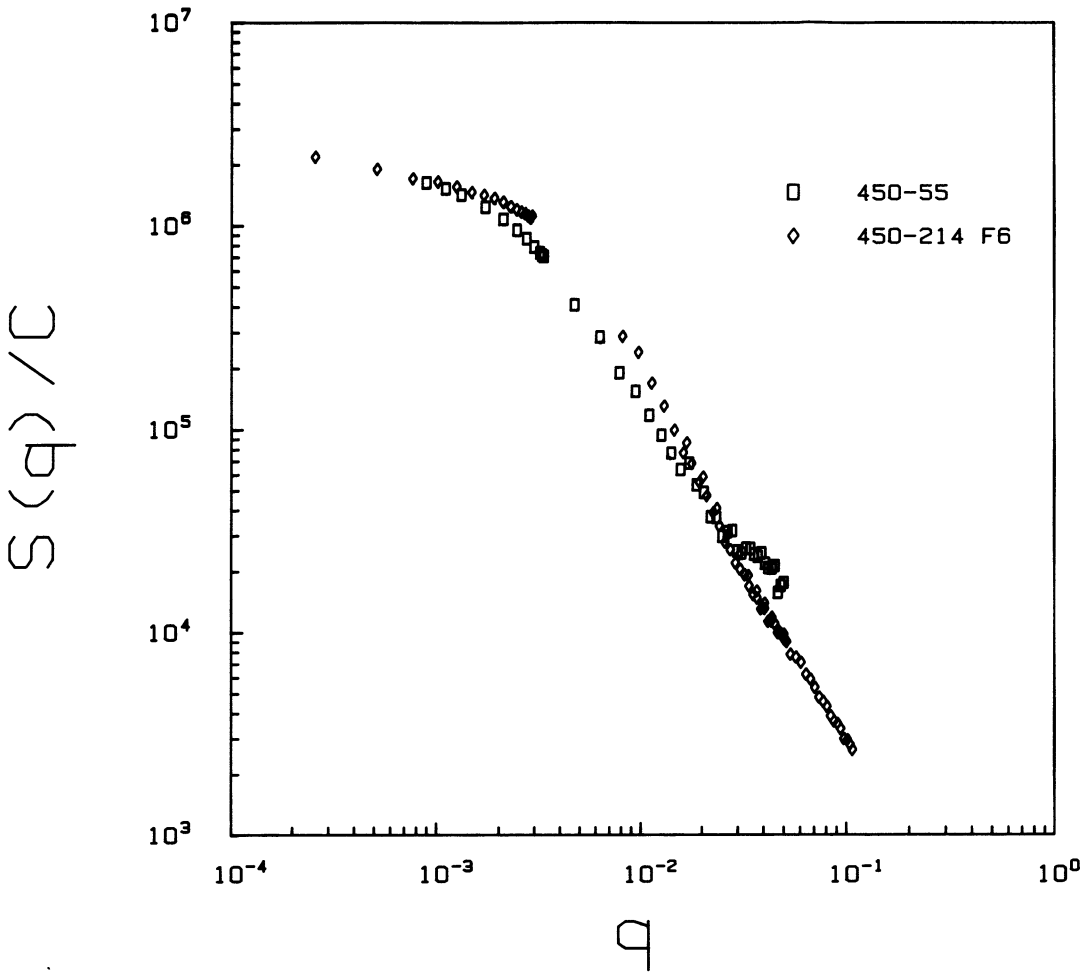


Fig. 4. — Comparison of the intensities scattered from polydisperse and fractionated samples with the same weight average molecular weight.

Using the values of $D_{app}$ and $D$ measured by the LS and SANS techniques, one can calculate the corresponding $\tau$ values, $\tau_{LS} = 2.18 \pm 0.08$ and $\bar{\tau} = 2.26 \pm 0.1$. They are consistent, although smaller, with the value $\tau_{SEC} = 2.3 \pm 0.1$ directly measured on some of these samples by the SEC-LALLS technique [6]. Table IV summarizes the results.

Previous work has shown that the size distribution functions of these samples obey the scaling form (5) [6]. Indirect arguments have also suggested that these pregels, assumed to be fractals, should have a fractal dimension close to 2 in dilute solutions [6, 9]. The results presented here sustain further the idea that these samples contain fractals objects. Moreover the values in table IV show that the behavior of these objects in solution is in good agreement with that expected for swollen percolation clusters.

Some evidence for the same behavior has been obtained on different systems [7, 8, 10-12, 17]. The values of the exponents measured here are in agreement within the experimental errors with those measured on pregels obtained by the end-linking of functionalized precursors chains [8] or by the polycondensation reaction of bi- and multifunctional units

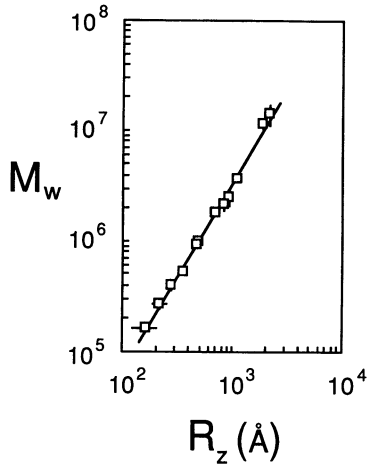


Fig. 5. — Same as figure 2 for the polydisperse pregels listed in table I.

Table IV. — *Mean experimental values of the exponents.*

| | LS | SANS |
|---|---|---|
| $D_{app}$ | 1.67 ± 0.04 | 1.53 ± 0.15 |
| $D$ | 2.04 ± 0.15 | 2.06 ± 0.10 |
| $D_\ell$ | — | 1.70 ± 0.05 |
| $\tau$ | 2.18 ± 0.08 | 2.26 ± 0.11 |

[7, 10-12, 17]. All these systems are characterized by a small ratio of branch points to monomer molar concentrations. This feature may explain that the simple static percolation model allows one to describe a variety of different gelling systems. However once the gelling reaction is completed, the mechanical properties of the resulting gels are quite different. For example it is well known that the upper limit of the stress before fracture is much smaller for gels obtained by end-linking than for gels synthesized by random crosslinking along the linear precursor chains. A simple model is still lacking to explain these differences.

**Acknowledgments.**

We are grateful to J. Teixeira, our local contact on the spectrometer Pace, for his help during the experiments. We thank him as well as J. Bastide, J. P. Cotton and M. Rawiso for sharing with us their experience in the SANS technique. We thank F. Candau for kindly giving access to her light scattering apparatus. Z. Mankowski made possible the $\gamma$-irradiation of sample 450-214 in the Co source available in Thiais.

## References


[1] See for instance :
Kinetics of Aggregation and Gelation, Eds. F. Family, D. P. Landau (North Holland) 1984 ;
Physics of Finely Divided Matter, Eds. M. Daoud, N. Boccara, *Springer Proc. Phys.* **5** (1985) ;
On Growth and Form, Eds. H. E. Stanley, N. Ostrowski, Martinus Nijhoff (1986).

[2] STAUFFER D., CONIGLIO A., ADAM M., *Adv. Polym. Sci.* (Springer Verlag, Berlin) 1982.

[3] STAUFFER D., *J. Chem. Soc., Faraday Trans. II* **72** (1976) 1354 ; *Phys. Rep.* **54** (1979) 1.

[4] DAOUD M., FAMILY F., JANNINK G., *J. Phys. Lett. France* **45** (1984) 199.

[5] MARTIN J. E., ACKERSON B. J., *Phys. Rev. A* **31** (1985) 1180.

[6] LEIBLER L., SCHOSSELER F., *Phys. Rev. Lett.* **55** (1985) 1110 ;
SCHOSSELER F., BENOIT H., GRUBISIC-GALLOT Z., STRAZIELLE C., LEIBLER L., *Macromolecules* **22** (1989) 400.

[7] PATTON E. V., WESSON J. A., RUBINSTEIN M., WILSON J. C., OPPENHEIMER L. E., *Macromolecules* **22** (1989) 1946.

[8] LAPP A., LEIBLER L., SCHOSSELER F., STRAZIELLE C., *Macromolecules* **22** (1989) 2871.

[9] SCHOSSELER F., LEIBLER L., *Macromolecules* **18** (1985) 398.

[10] BOUCHAUD E., DELSANTI M., ADAM M., DAOUD M., DURAND D., *J. Phys. Lett. France* **47** (1986) 1273.

[11] ADAM M., DELSANTI M., MUNCH J. P., DURAND D., *J. Phys. France* **48** (1987) 1809.

[12] MUNCH J. P., ANKRIM M., HILD G., OKASHA R., CANDAU S. J., *Macromolecules* **17** (1984) 110 ;
CANDAU S. J., ANKRIM M., MUNCH J. P., REMPP P., HILD G., OKASHA R., in Physical Optics of Dynamic Phenomena and Processes in Macromolecules Systems, W. de Gruyter, Berlin (1987).

[13] MANDELBROT B. B., The Fractal Geometry of Nature, Freeman, San Francisco (1982).

[14] The Fractal Approach to Heterogeneous Chemistry, Ed. D. Avnir, J. Wiley (1989).

[15] WITTEN T. A., SANDER L. M., *Phys. Rev. Lett.* **47** (1981) 1400.

[16] STOCKMAYER W. H., *J. Chem. Phys.* **11** (1943) 45 ; **12** (1944) 125 ;
FLORY P. J., Principles of Polymer Chemistry (Cornell University Press, Ithaca, NY) 1976.

[17] SCHMIDT M., BURCHARD W., *Macromolecules* **14** (1981) 370.